Femtosecond laser ablation properties of borosilicate glass

Adela Ben-Yakar[a)]

Mechanical Engineering Department, The University of Texas at Austin, Austin, Texas 78712; and Applied Physics Department, Ginzton Lab, Stanford University, Stanford, California 94305

Robert L. Byer

Applied Physics Department, Ginzton Lab, Stanford University, Stanford, California 94305

We study the femtosecond laser ablation properties of borosilicate glass using atomic force microscopy and laser pulses of 200 fs duration, centered at 780 nm wavelength. We show that both single-shot and multishot ablation threshold fluences can be determined by studying the diameter and the depth of single-shot ablated craters. The linear relationship between the square of the crater diameter and the logarithm of the laser fluence in the form of $D^2 = 2w_0^2 \ln(F_0/F_{th}^{N=1})$ provides the single-shot ablation threshold, $F_{th}^{N=1}$, whereas the linear relationship between the ablation depth and the logarithm of laser fluence in the form of $h_a = \alpha_{eff}^{-1} \ln(F_0/F_{th}^{N>1})$ provides the multishot ablation threshold, $F_{th}^{N>1}$. The results depict a multishot ablation threshold of ≈ 1.7 J/cm^2 independent of the atmospheric conditions. The slopes of the linear fits also provide a precise estimate of the beam radius at the surface, $w_0 \approx 5.9$ μm, and the "effective optical penetration depth," $\alpha_{eff}^{-1} \approx 238$ nm in air. The method is systematic, provides results that are consistent with the literature, and eliminates uncertainties because of instrument sensitivities. We also show that threshold measurement based on the extrapolation of volume to zero, a method used often in previous studies, is somewhat questionable. Finally, the measured dimensions of ablated craters reveal that the ablation volume per unit input energy is about 1.3–1.5 μm^3/μJ at an intermediate fluence regime of $10 < F_0^{av} < 40$ J/cm^2. This value represents an order of magnitude larger ablation efficiency when compared to the ablation of glass with nanosecond ultraviolet laser pulses. © *2004 American Institute of Physics.* [DOI: 10.1063/1.1787145]

I. INTRODUCTION

A well-controlled femtosecond laser micromachining process requires a thorough characterization of the ablation properties of the substrate, such as the ablation threshold and the ablation rate. We present a detailed examination of the femtosecond laser ablation properties of borosilicate glass. This wide band gap dielectric material is advantageous for microfluidic devices because of its high thermal and chemical stability, low conductivity, and low transmission loss in optical detection.

Micromachining of wide band gap dielectrics using femtosecond lasers is a nearly wavelength independent ablation process. High peak intensities associated with ultrashort laser pulses provide large photon fluxes necessary to initiate nonlinear absorption processes (multiphoton initiated avalanche ionization).[1] Ablation takes place when the density of free conduction band electrons (CBE) reaches a critical density. This happens above a certain laser fluence threshold at which point the electrostatic forces are high enough to break down the material and to eject the ionized nuclei. The minimum laser fluence below which ablation cannot be initiated is defined as the ablation threshold or optical breakdown threshold.

Several studies have measured the optical breakdown threshold of various dielectric materials such as fused silica,[1–5] calcium fluoride (CaF$_2$),[2,4] and barium aluminum borosilicate glass[3,6] when exposed to ultrashort laser pulses. The most significant observation was deviation from the $\sqrt{\tau}$ dependence of the damage threshold, where τ is the pulse duration. In the long-pulse regime ($\tau > 10$ ps), the process is controlled by the rate of thermal conduction through the atomic lattice[7] that scales with $\sqrt{\tau}$. In the short-pulse regime ($\tau < 10$ ps), the optical breakdown is a nonthermal process and various nonlinear ionization mechanisms (multiphoton, avalanche, tunneling) become important. Damage threshold still shows a decreasing trend with τ, however, with a weaker dependence.[2,3] Below 100 fs, multiphoton ionization is primarily responsible for optical breakdown where a steeper decrease of the threshold fluence with τ has been reported.[3]

Some groups have examined the effect of material band-gap and laser wavelength on damage threshold.[2,3,8] Stuart *et al.*,[2] for example, showed that short pulse (400 fs) damage thresholds in various fluorides scale with band gap energy, as expected from multiphoton initiated avalanche ionization. They also observed a decrease by roughly a factor of 2 in the damage threshold in fused silica for 526 nm pulses compared to 1053 nm pulses for pulse durations of 300 fs and longer.[2]

Atmospheric pressure and gas conditions at which the material is ablated have an effect on damage threshold. When irradiated in vacuum, certain dielectrics showed a reduction in multishot damage threshold. This effect has been observed in fused silica exposed to 355 nm, 10 ns laser

[a)]Author to whom correspondence should be addressed: electronic mail: ben-yakar@mail.utexas.edu

pulses[9] as well as in crystalline quartz[10] and is attributed to the reduction of SiO_2 in the vacuum environment.

Many different criteria have been used to define damage threshold. Lenzer et al.[3] measured the volume of material ablated with 50 laser pulses and extrapolated to zero ablated volume to obtain a threshold. In contrast, Rosenfeld et al.[4] used an in situ scattering light technique to detect the surface damage. Kautek et al.[6] used both in situ and ex situ techniques including observation of visible damage by speckle formation in the transmitted He-Ne laser beam and extrapolation of volume of multishot ablated material to zero. The damage threshold results varied between different methods and groups. The measurements were influenced by instrument sensitivity and by the precision of threshold fluence (beam radius) quantification at the surface.

Here, we present a consistent and systematic way of determining a variety of parameters by measuring only the dimensions of craters ablated with a single femtosecond laser pulse. These parameters include the ablation threshold, the effective absorption coefficient, and the beam diameter at the laser/material interaction plane.

II. EXPERIMENTAL DETAILS

We carried out the experiments on a 1.1 mm thick borosilicate glass sample (Precision Glass and Optics, Ltd.). The chemical composition of borosilicate glass (also known as Corning 7740) is 81% SiO_2, 13% B_2O_3, 2% Al_2O_3, and 4% Na_2O and its band gap energy is about $E_b \approx 4$ eV.[3] The glass substrates were cleaned ultrasonically with methanol before and after the experiments.

The laser pulses with a $\tau = 200$ fs pulse duration and a $\lambda = 780$ nm center wavelength were generated using a regeneratively amplified Ti:sapphire laser. We measured the laser beam quality at the amplifier output in terms of the "M-squared" parameter[11] and found that $M^2 = 1.8 \pm 0.2$. The experiments were performed both in air at atmospheric pressure and in vacuum at pressures below 10^{-4} mbar. The surface of the samples was positioned to be normal to the direction of the incident beam. We measured the energy losses along the beam path including the losses through the glass window of the vacuum chamber. Owing to the long working distance of the objective lens the window of the vacuum chamber could be placed far from the sample surface. This way, we did not observe any significant deposition of the ablated material on the windows.

A linearly polarized laser beam with a $1/e^2$ radius of $w_0 = 5.9 \pm 0.1$ μm was delivered to the surface by a long working distance objective lens (Mitutoya, 5x, NA=0.14) attached to a microscope. To obtain a homogeneous and well-defined distribution on the target, a circular aperture (5.5 mm in diameter) was placed in the beam path just before the objective lens. We verified that the truncation of the laser beam, originally 7 mm in diameter, did not cause any significant modulation of the spatial beam profile at the sample surface. To do this, we calculated the energy density of the modulated Gaussian beam at the focal plane of the objective lens using[8,12]

$$F(r) = \frac{2E_{pulse}k^2}{\pi} \int_0^{a/w_0} \rho \exp(-\rho^2) J_0(kr\rho) d\rho, \qquad (1)$$

where E_{pulse} is the total pulse energy, $k = 2\pi w_0/f\lambda$ is defined as a characteristic inverse length, a is the radius of the truncated aperture, f is the focal length of the lens, ρ is the radial distance from the center of the pulse, and J_0 is the zero-order Bessel function. We found that the calculated energy density in the sidebands of the distribution was less than 1% of the maximum fluence. Therefore, we could assume that the focused beam on the target surface had a Gaussian spatial beam profile with a negligible energy density fluctuations.

Following the ablation, we measured the three-dimensional profile (depth and diameter) of the single-shot craters using an atomic force microscope (AFM), which is shown to be an excellent tool to investigate craters with depths less than 6 μm.

III. RESULTS AND DISCUSSION

Figure 1(a) presents three AFM images of craters ablated in vacuum with a single laser pulse of different energies; 13.8, 18.8, and 30 μJ. The images show a smooth center surrounded with an elevated rim from which thin strips of melted material are extending away. This rim is the origin of the rough laser micromachined surfaces. In a detailed study of the formation mechanism of the rim,[13] we have shown that a thin molten region forms during the ablation process. An elevated rim seems to form as a result of a pressure driven flow of the melt from the center to the edge of the crater followed by resolidification at the rim.

The cross-sectional profiles at the centerline of the craters are plotted in Fig. 1(b). To show the details of the shallow profiles, we present the y axis (depth) in nanometers and the x axis (radial position) in micrometers. When defined in terms of the laser wavelength λ, the craters are $\sim \lambda/2$ deep and $\sim 15\lambda$ wide in diameter for the laser energies and focusing conditions used in current experiments. Both widening and deepening of the craters appear for increasing laser fluences. The rim surrounding the crater is higher than the surface by $\sim \lambda/10$ and becomes slightly higher with increasing laser fluences.

Figures 2 and 3 present the measured values of the ablation diameter D and the ablation depth h_a of craters exposed to different laser fluences. The figures include two sets of data from experiments performed in air and in vacuum. In the experiments performed in air, the last four experimental points in the high-fluence regime show a divergence from the expected linear increase. This indicates the nonlinear beam distortion in air due to the air breakdown at high laser fluences. The formation of an air plasma blocks the energy reaching the ablation surface and therefore reduces the ablation rate. In the calculation of ablation parameters, we excluded these last four data points to avoid the effect of the beam distortion in air.

We next discuss how to determine the ablation parameters by measuring the dimensions of single-shot craters.

5318   J. Appl. Phys., Vol. 96, No. 9, 1 November 2004

A. Ben-Yakar and R. L. Byer

(a)

$E_{pulse} = 13.8\ \mu J$ $E_{pulse} = 18.8\ \mu J$ $E_{pulse} = 30.0\ \mu J$
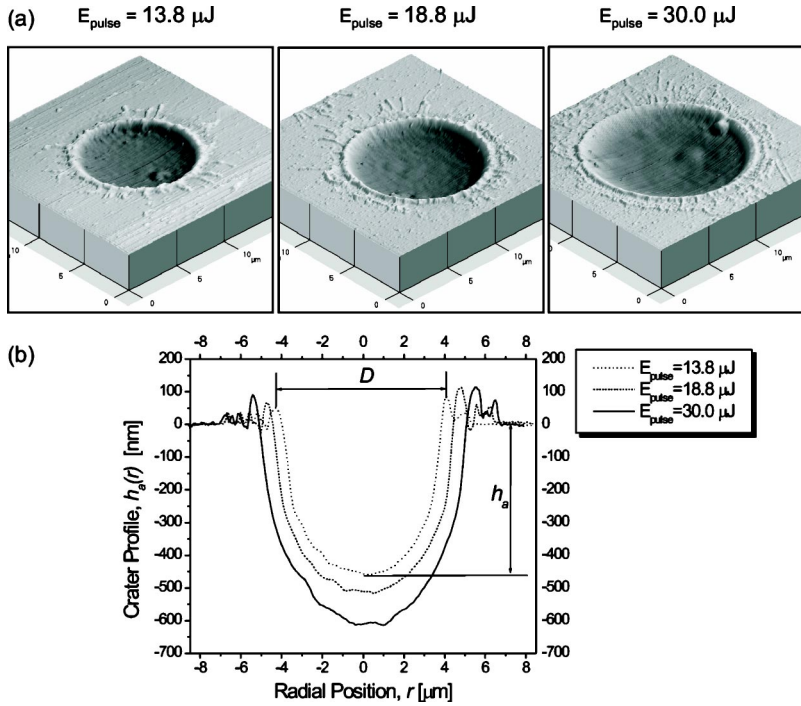

(b)

FIG. 1. Quantitative evaluation of single-shot laser ablated craters using an atomic force microscope. (a) Three-dimensional AFM images of single-shot craters ablated in vacuum with three different laser pulse energies, E_{pulse}=13.8, 18.8, and 30.0 μJ corresponding to laser fluences of F_0^{av}=13.1, 17.9, and 28.6 J/cm², respectively. The diameter of the craters increases with laser energy. (b) Center-line profiles of the ablated craters. The crater diameter D and the crater depth h_a were measured from data similar to the profiles presented here. The diameter is taken as the distance across the highest points of the rim and the ablation depth is measured from the surface to the bottom of the crater as illustrated in the graph. Note that the scale in the lateral direction is 10 times larger than in the direction normal to the target surface.

A. Single-shot ablation threshold

The "single-shot ablation threshold" $F_{th}^{N=1}$ represents the minimum average laser fluence required to initiate ablation with the first laser pulse. We determine $F_{th}^{N=1}$ by measuring the crater diameter D for different average laser fluences F_0^{av} and by using the linear relationship between D^2 and $\ln(F_0^{av})$ that can be derived as follows.

For a Gaussian spatial beam profile with a $1/e^2$ laser beam radius w_0 the radial distribution of the laser fluence is presented by

$$F(r) = F_0^{peak}\exp\left(-\frac{2r^2}{w_0^2}\right),\tag{2}$$

where F_0^{peak} is the peak laser fluence. Substituting $r=D/2$ and recognizing that the material cannot be ablated for laser fluences lower than the threshold (namely, $D=0$ at the threshold laser fluence, $F_0^{peak}=F_{th}$), we obtain[14]

$$D^2 = 2w_0^2 \ln\left(\frac{F_0^{peak}}{F_{th}}\right).\tag{3}$$

The peak laser fluence F_0^{peak} is related to the total pulse energy E_{pulse} according to

$$F_0^{peak} = \frac{2E_{pulse}}{\pi w_0^2},\tag{4}$$

because E_{pulse} is the integrated value of the Gaussian profile of laser fluence over the irradiated area with a radius w_0. In the literature, most studies report the fluence in terms of an average value defined by
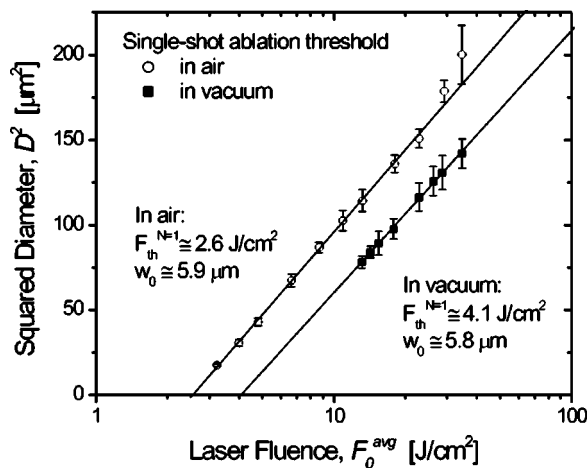

FIG. 2. The single-shot ablation threshold measurements of borosilicate glass with laser pulses of λ=780 nm and τ=200 fs. The squared diameter D^2 of the ablated areas is plotted as a function of the laser fluence F_0^{av}. The slope of the linear fit [Eq. (6)] yields the beam radius at the surface, w_0, and the extrapolation to zero provides the single-shot ablation threshold $F_{th}^{N=1}$.
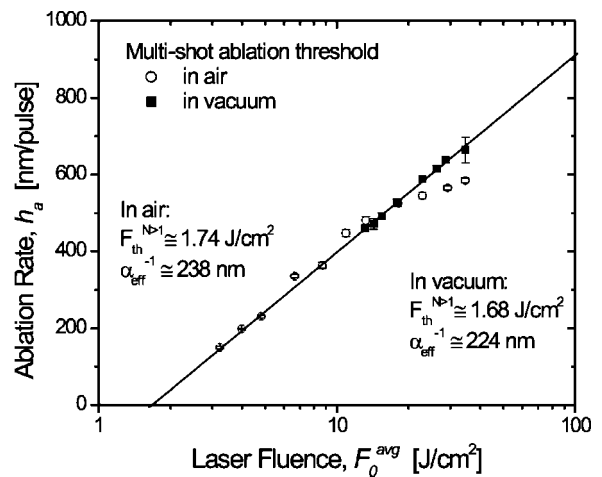

FIG. 3. The multishot ablation threshold measurements of borosilicate glass with laser pulses of λ=780 nm and τ=200 fs. The plots present the logarithmic dependence of the ablation rate h_a on the laser fluence F_0^{av}. The slope of the linear fit [Eq. (10)] can be interpreted as the effective optical penetration depth α_{eff}^{-1}. The extrapolation to zero provides the multishot ablation threshold $F_{th}^{N>1}$.

$$F_0^{\mathrm{av}} = \frac{E_{\mathrm{pulse}}}{\pi w_0^2}. \tag{5}$$

Note that there is a factor of 2 difference between peak and average laser fluences for a Gaussian beam. To be consistent with the literature, we used F_0^{av} in describing the laser fluence. The slope of Eq. (3) remains unchanged if F_0^{av} is used instead of F_0^{peak} and we obtain

$$D^2 = 2w_0^2 \ln\left(\frac{F_0^{\mathrm{av}}}{F_{\mathrm{th}}^{N=1}}\right), \tag{6}$$

where N is the number of laser pulses. Figure 2 shows this linear relation between the squared diameter and the logarithm of the average laser fluence in our measurements. The extrapolation of the linear fit [Eq. (6)] to $D^2=0$ results in a single-shot ablation threshold of $F_{\mathrm{th}}^{N=1}=4.06\pm0.06$ J/cm^2 in vacuum and a lower value of $F_{\mathrm{th}}^{N=1}=2.55\pm0.04$ J/cm^2 in air.

The other parameter that can precisely be obtained from D^2 measurements is the beam radius w_0 at the interaction surface. In order to estimate the average fluence, the precise knowledge of w_0 is required. Since it is easier to measure E_{pulse} experimentally, we replace the fluence ratio in Eq. (6) by the ratio of the pulse energies, yielding

$$D^2 = 2w_0^2 \ln\left(\frac{E_{\mathrm{pulse}}}{E_{\mathrm{th}}}\right). \tag{7}$$

The beam radius focused on the surface can now be determined by estimating the slope of this linear fit to data points. We obtain a $1/e^2$ Gaussian beam radius of $w_0=5.78$ and 5.92 μm for the experiments in vacuum and in air, respectively, for the 5× objective lens. Because the measured Gaussian spot size on the surface is not necessarily equal to the calculated spot size at the focal point of the objective, this technique provides a convenient means for determining the exact Gaussian beam spot size at the interaction surface.

B. Multishot ablation threshold

The ablation threshold is expected to decrease for increasing number of overlapping pulses due to material dependent "incubation effect".[4,5,15] The incubation effect is attributed to surface defects generated by the interaction of multiple laser pulses with fluences lower than the single-shot ablation threshold. These defects are the results of the changes in the mechanical and/or chemical properties of the material and can lead to ablation at lower threshold values. The most dramatic decrease in the ablation threshold is observed typically during the first 20 laser shots. Rosenfeld et al.,[4] for example, obtained a 75% decrease in the damage threshold of fused silica: a single-shot damage threshold of 3.7 J/cm^2 reduced to 0.9 J/cm^2 when 20 laser pulses were used.

To take into account the incubation effect, multishot ablation threshold is usually determined by analyzing the diameter of ablation craters generated with multiple laser pulses (usually $N=50$ pulses). It has been shown that the linear relationship between the square of the crater diameter and the logarithm of the laser fluence given in Eq. (6) is valid in the case of multishot craters as well.[16] However, it has also been showed that the accuracy of D^2 measurement in the multishot experiments is substantially diminished due to cracks appearing around the craters.[17] When exposed to a certain number of laser pulses, the mechanical properties of glass are modified by the low fluence laser beam around the ablated area and relatively large cracks may appear even when using pulses as short as 100 fs.

Another way of calculating the multishot ablation threshold is to use the logarithmic dependence of the ablation rate d on the laser fluence as described by[18,19]

$$d = \alpha_{\mathrm{eff}}^{-1} \ln\left(\frac{F_0^{\mathrm{av}}}{F_{\mathrm{th}}^{N>1}}\right). \tag{8}$$

Here, $\alpha_{\mathrm{eff}}^{-1}$ can be interpreted as the "effective optical penetration depth" as expected from the *Beer-Lambert law*. Once the steady state material removal is established after a few incubation pulses, the depth of the ablated material, h_a, increases linearly with the number of laser pulses according to[6,15,20]

$$h_a = d(N - N_{\mathrm{th}}). \tag{9}$$

Here, the number of incubation pulses N_{th} represents the minimum number of laser pulses to initiate ablation and its value depends on the laser fluence, close to the threshold $N_{\mathrm{th}}=50$ and well above the threshold $N_{\mathrm{th}}=0$.

The ablation rate d is usually determined by measuring the ablation depth of multishot craters and dividing it by the number of pulses according to Eq. (9). However, it might be difficult to measure the ablation depth of multishot craters with high precision because multiple pulses can create deep craters (>6 μm) beyond the working range of AFM. Also, the validity of Eq. (9) is questionable when using a laser beam with a small diameter ($2w_0<10$ μm) because high aspect ratios (beyond the 1:1 ratio) can be achieved within the first 10–15 pulses. The difficulty in removing material from deep craters due to the plasma confinement reduces the ablation rate with increasing number of pulses. Hence, the dependence of h_a on N begins to depart from the linear law given in Eq. (9).

An easier and more precise way of determining the multishot ablation threshold is to measure the depth of single-shot craters ablated with laser fluences well above the threshold for which $N_{\mathrm{th}}=0$.[4] This means that the steady state material removal begins with the first pulse and the ablation rate will thus be equal to the single-shot ablation depth, $d=h_a^{N=1}$.

In the current paper, we therefore propose to use the depth of the single-shot ablated craters in estimating the multishot ablation threshold. Since we use laser fluences well above the threshold, $N_{\mathrm{th}}=0$, we can substitute $d=h_a$ in Eq. (8) resulting in,

$$h_a = \alpha_{\mathrm{eff}}^{-1} \ln\left(\frac{F_0^{\mathrm{av}}}{F_{\mathrm{th}}^{N>1}}\right). \tag{10}$$

Figure 3 shows this linear relationship between the single-shot ablation depth and the logarithm of laser fluence. The extrapolation of the linear fit to zero provides a multishot ablation threshold of $F_{\mathrm{th}}^{N>1}=1.68\pm0.03$ J/cm^2 in vacuum and $F_{\mathrm{th}}^{N>1}=1.74\pm0.02$ J/cm^2 in air. These values are in good

agreement with previous multishot damage threshold measurements for borosilicate glass.[6,16] This consistency suggests that the simple technique proposed here is a valid technique for measuring the multishot ablation threshold.

C. Optical absorption coefficient

The optical absorption coefficient α_{eff} of a material determines the vertical (depth) precision of the ablation process. In general, a larger α_{eff} results in a smaller optical penetration depth and thus better control of the ablation depth. The nonthermal ablation process with femtosecond laser pulses takes place in a volume primarily determined by this parameter.

As discussed in the preceding section, the slope of the linear relation given in Eq. (10) can be interpreted as the effective optical penetration depth, $\alpha_{eff}^{-1}=1/\alpha_{eff}$. The slope of the linear fit to data points provides $\alpha_{eff}^{-1}=224$ nm in vacuum and 238 nm in air which corresponds to an effective absorption coefficient of $\alpha_{eff}=4.5\times10^4$ and 4.2×10^4 cm^{-1} in vacuum and in air, respectively.

These measured optical absorption coefficients are about 30 times larger than the effective absorption coefficient of borosilicate glass when exposed to a 10 ns, 266 nm laser pulses ($\alpha_{eff}=1.5\times10^3$ cm^{-1}, $\alpha_{eff}^{-1}=6.7$ μm).[16] However, it is comparable to the effective absorption coefficient of fused silica when exposed to 15 ns, 157 nm F$_2$-laser pulses ($\alpha_{eff}=1.7\times10^5$ cm^{-1}, $\alpha_{eff}^{-1}=59$ nm).[21] This suggests that the combination of ultrashort pulses ($\tau\lesssim1$ ps) with near-infrared (NIR) / visible wavelengths (780 nm) results in a comparable absorption properties to those obtained with the application of long pulses ($\tau>1$ ns) with vacuum-ultraviolet (VUV) wavelengths (157–196 nm).

The similarity in the absorption properties between NIR femtosecond lasers and VUV nanosecond lasers indicates that both lasers can provide the depth control necessary for high precision in micromachining of wide band gap dielectrics. Among those, femtosecond lasers might demonstrate an advantage with their well-controlled Gaussian beam shape for direct writing and high-aspect ratio etching applications. However, VUV nanosecond lasers seem to provide a better control of the surface roughness.[21]

These unique absorption properties of borosilicate glass at the NIR/visible wavelengths could be explained in terms of the density of the free electrons. Borosilicate glass has a very weak linear absorption coefficient at the NIR/visible wavelengths. In the femtosecond regime, however, high peak intensities can initiate nonlinear absorption processes (multiphoton initiated avalanche ionization) generating a high density of free electrons in the conduction band within a thin surface layer.[1,2] The optical penetration depth mainly depends on the diffusion length of these CBE. CBE velocity is of the order of 1 nm/fs.[22] Considering the CBE diffusion happens in the time range that is the sum of the pulse duration ($\tau=200$ fs) and the CBE lifetime [$t_{life}=150$ fs (Ref. 23)], we obtain CBE diffusion length of the order of 350 nm.[20] This value is a bit higher than the measured optical penetration depth. On the other hand, it has been shown that when the incident intensity is high enough, main absorption occurs

early in the pulse and the rest of the incoming energy is reflected back due to the critical density plasma that serves as a mirror.[1] Since the critical density plasma for the laser intensities used in our experiments is formed in the first half of the pulse ($\tau/2=100$ fs), we obtain a CBE diffusion length of the order of 250 nm ($\tau/2+t_{life}$). Thus, we can conclude that the α_{eff}^{-1} can be related to the CBE diffusion length.

D. Ablation volume and efficiency

Most previous studies estimate the ablation volume V by assuming a flat bottom for the ablated crater so that $V=\pi D^2/4h_a$. However, because of the Gaussian beam profile, the actual ablation profile has a curvature as shown in Fig. 1(b). In this paper, we calculate the single-shot ablated crater volume by integrating the volume elements enclosed by the measured crater profile and the undisturbed plane:

$$V=2\pi\int_0^{D/2}rh_a(r)dr,\tag{11}$$

where r is the radial distance from the center of the crater.

Figures 4(a) and 4(b) present the actual ablation volume estimated using Eq. (11) and the one estimated simply by using $V=\pi D^2/4h_a$ as a function of laser fluence. The results show that the actual volume is about 50%–60% of the volume estimated using $V=\pi D^2/4h_a$. The data also show a nonlinear dependence of the ablation volume on the logarithm of the laser fluence. This nonlinearity is particularly clear in Fig. 4(a) where the data points are spread out on a broader fluence range.

The ablation volume is expected to scale linearly with the squared logarithm of the laser fluence because it consists of two parameters, D^2 and h_a, each separately depending on the logarithm of the fluence. Figure 4(c) demonstrates this linearity between the volume and the squared logarithm of the laser fluence. It is surprising that most of the earlier investigators determined the threshold fluence by assuming a linear relationship between the ablation volume and the logarithm of the laser fluence and that they achieved reasonable values by extrapolating the linear fit to zero.[3,5,6,16]

From micromachining point of view, it is important to know how much volume is ablated per unit input energy. Figure 5 (right axis) shows the ratio of the ablated volume per incident total pulse energy as a function of laser fluence. The results indicate that the amount of material removal per unit energy is nearly constant at an intermediate fluence regime of $10<F_0^{av}<40$ J/cm^2 and is about 1.3 μm$^3/\mu$J in vacuum and 1.5 μm$^3/\mu$J in air. Namely, a volume of 1.3–1.5 μm^3 can be ablated with a 1 μJ of 200 fs laser pulse energy. This value represents an order of magnitude higher efficiency when compared to the energy consumption of borosilicate glass ablation with 10 ns, 266 nm laser pulses.[16] Femtosecond laser pulses provide optimum energy deposition in the volume of the target material because energy dissipation from the absorption zone occurs on a time scale significantly longer than laser pulse duration.

We can now define an ablation efficiency η in terms of the ratio of the energy required to heat a unit volume to melting point to the energy required to ablate a unit volume,
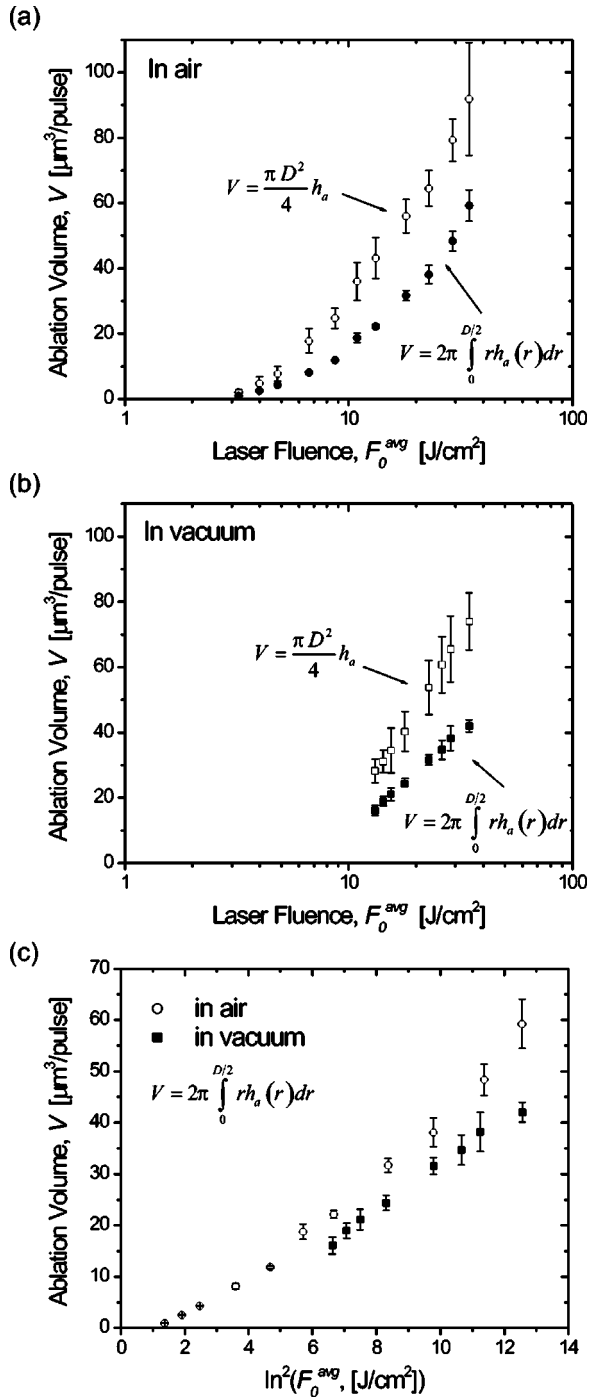
FIG. 5. The right axis of the plot shows the ablation volume per unit input energy (V/E_{pulse}). The left axis of the plot shows the ablation efficiency [$\eta = \rho C_p (T_m - T_0) V / E_{\mathrm{pulse}}$], described in Eq. (12) in terms of the ratio of the energy required to heat the ablation volume to the melting point to the incident pulse energy. Note that the left and right axes are proportional.

Namely, in average only $\approx 0.47\%$ of the input energy is used to melt the ablation volume. Most of the absorbed energy is actually used to remove the ablated material from the surface by the hydrodynamic expansion[26] of the plasma.

The ablation efficiency could also be defined in comparison to heat of vaporization of silica instead of heat of melting. The energy required to melt 1 cm^3 of silica is approximately 3.4 kJ (using the values given above), while the energy required to vaporize 1 cm^3 of silica is about 18.3 kJ.[27] Thus, the ablation efficiency described in terms of heat of vaporization would be five times lower than the one described in terms of heat of melting.

The results show that the ablation is less efficient when the incident laser fluence is close to the threshold. This contradicts the fact that the reflectivity of dielectrics decreases at low laser fluences. The measurements of Perry et al.[1] showed that when glass is exposed to fluences well above threshold ($F_0 > 5-10 F_{\mathrm{th}}$), a large portion of the incident energy is reflected back from the sample. Consequently, an increased ablation efficiency is expected when using low laser fluences, as shown in the case of the ablation of metals.[28] However, in glass materials, the decrease in reflectivity at low fluences does not necessarily indicate that the absorptivity is increased, because it may be possible that the transmissivity of near-IR light through glass is increased. The reduced ablation efficiency at low laser fluences may be attributed to a decrease of the glass surface absorptivity within the ablation layer.

E. Effect of processing environment: Air vs vacuum

Little is known about the influence of the processing environment on the properties of femtosecond laser ablation of glass. Our study indicates that there is a slight dependence on the processing environment when using single-shots (a lower fluence is required to initiate ablation in air) and there is not any significant dependence when using multiple shots.

The lower single-shot ablation threshold in air can possibly be attributed to the modified absorption process. First, the reactive environment (air) could accelerate the ablation

FIG. 4. The volume of the ablated craters (a) as a function of the average laser fluence in air and (b) in vacuum and (c) as a function of the squared logarithm of the laser fluence.

$$\eta = \frac{\rho C_p (T_m - T_0)}{E_{\mathrm{pulse}}/V}, \qquad (12)$$

where $\rho = 2.23 \times 10^3$ kg/m^3 (Ref. 24) is the density, $C_p = 1250$ J/kg K (Ref. 25) is the specific heat at an average temperature of $T = 900$ K, $T_0 = 300$ K is the initial temperature, and $T_m = 1500$ K (Ref. 24) is the working point of glass, defined as the melting temperature at which the glass can be easily formed and sealed. As Fig. 5 (left axis) shows, these values yield an ablation efficiency of $\eta \approx 0.51\%$ in air and $\eta \approx 0.43\%$ in vacuum for intermediate laser fluences.
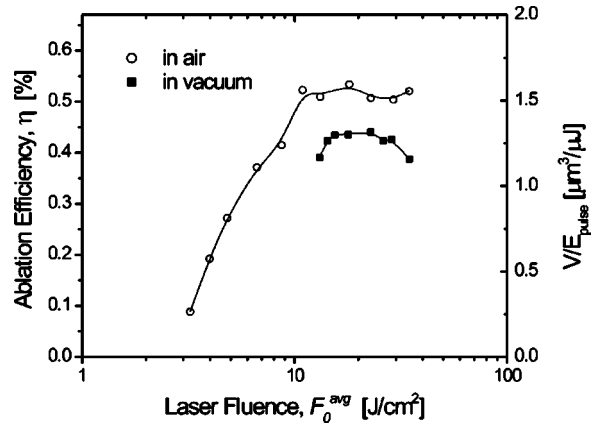
chemistry. Second, the hot plasma in air expands at a slower speed than in vacuum due to air resistance. Slow expansion provides a longer time for the energy to couple from plasma radiation into the target. Both of these reasons could lead to a modified absorption and thus a reduced threshold fluence to initiate ablation in air when using a single laser pulse.

When multiple pulses overlap, the resulting incubation effect apparently reduces the dependence on the processing environment. A supporting and independent experiment was performed by Plettner[29] who observed no difference between multishot damage threshold in air and in vacuum for borosilicate glass and also for fluorides (CaF_2 and BaF_2). However, for fused silica exposed to 355 nm, 10 ns laser pulses[9] as well as for crystalline quartz,[10] the multishot ablation threshold was found to drop in vacuum. The mechanism for this phenomena was investigated previously and attributed to the reduction of SiO_2, namely to the formation of SiO_x where $x<2$, in vacuum conditions. Laser irradiation in air apparently drives the photochemical oxidation reaction back to SiO_2. However, neither our study nor the study of Plettner[29] showed any indication for the existence of this phenomena in borosilicate glass. Another reason for this phenomena might be related to the formation of a hydrated (water) layer on the surface and to the difficulty in removing it from borosilicate glass. It is possible that if we leave the samples in vacuum for an extended period of time, we can remove the hydrated layer from the surface. In this case, borosilicate glass might demonstrate properties similar to fused silica.

The ablation rate of borosilicate glass was also found to be independent of the processing environment. The energy deposition is governed by the optical penetration depth that is mainly dependent on the diffusion length of the CBE. This is however valid only for the surface ablation. When ablating deep holes, the ablation rate might drop due to nonlinear effects in air. For example, ablation products that cannot escape the holes can cause self-focusing of incoming laser pulses even at powers lower than the critical power for self-focusing in ambient air.[30] A similar phenomena was observed for metals having greatly reduced ablation rates in air.[31]

A combined effect of the above factors leads to a slightly higher ablation efficiency in air (0.51% in air vs 0.43% in vacuum). One might have expected a higher efficiency in vacuum because of the less work required for the hydrodynamic expansion of plasma in a nonresistant environment. However, since the single-shot ablation threshold is lower in air, a larger diameter can be ablated in air. On the other hand, the ablation depth is independent of the processing environment since it is mainly determined by the optical penetration depth. Therefore, the resulting ablation volume is slightly higher in air. This indicates that the efficiency is mainly determined by the way energy is deposited into the material, and not by how the material is removed from the ablated target.

IV. CONCLUSIONS

We have investigated the femtosecond laser ablation properties of borosilicate glass by examining the single pulse craters using AFM. We determined both single-shot ($N=1$)

and multishot ($N>1$) ablation thresholds from the measurements of diameter and depth of the craters ablated with a single laser pulse. The extrapolation of the linear relationship between the square of crater diameter and the logarithm of laser fluence [Eq. (6)] to zero provides the single-shot ablation threshold, $F_{th}^{N=1}$. Whereas the extrapolation of the linear relationship between the ablation depth and the logarithm of laser fluence [Eq. (10)] to zero provides the multishot ablation threshold, $F_{th}^{N>1}$. The beam diameter at the interaction surface, w_0, and the effective optical penetration depth, α_{eff}^{-1}, can also be determined precisely from the slope of these linear relationships.

The results showed that ablation of borosilicate glass in air requires a lower threshold fluence than ablation in vacuum (about 2.6 J/cm^2 in air vs 4.1 J/cm^2 in vacuum) when using a single laser pulse. In the case of multiple pulses, however, no difference was observed (about 1.7 J/cm^2 both in air and vacuum). A modified absorption process could be responsible for the lower threshold when using single pulses. Since the multishot ablation threshold is already reduced due to the incubation effect, the processing environment has a minimal effect on the threshold value.

The proposed technique relies on the use of fluences well above threshold and on the fact that once steady state material removal is established, the depth of the ablated material increases linearly with the number of laser pulses at a given laser fluence. The method is systematic, provides results that are consistent with the literature, and eliminates uncertainties resulting from instrument sensitivities. The knowledge of exact beam diameter at the surface also provides a precise estimate of the laser fluence at the laser/material interaction surface.

Finally, we have calculated the volume of the ablated craters and the energy efficiency of femtosecond laser ablation of glass. The amount of material removal per unit energy is about 1.3–1.5 $\mu m^3/\mu J$ at an intermediate fluence regime of $10<F_0^{av}<40$ J/cm^2. This value represents an order of magnitude higher efficiency when compared to the energy required to ablate borosilicate glass with nanosecond UV laser pulses.

[1]M. D. Perry, B. C. Stuart, P. S. Banks, M. D. Feit, V. Yanovsky, and A. M. Rubenchik, J. Appl. Phys. **85**, 6803 (1999).
[2]B. C. Stuart, M. D. Feit, S. Herman, A. M. Rubenchik, B. W. Shore, and M. D. Perry, Phys. Rev. B **53**, 1749 (1996).
[3]M. Lenzner, J. Krüger, S. Satania, Z. Cheng, C. Spielmann, G. Mourou, W. Kautek, and F. Krausz, Phys. Rev. Lett. **80**, 4076 (1998).
[4]A. Rosenfeld, M. Lorenz, R. Stoian, and Ashkenazi, Appl. Phys. A: Mater. Sci. Process. **69**, S373 (1999).
[5]M. Lenzner, J. Krüger, W. Kautek, and F. Krausz, Appl. Phys. A: Mater.

Sci. Process. **69**, 465 (1999).

[6]W. Kautek, J. Krüger, M. Lenzner, S. Sartania, C. Spielmann, and F. Krausz, Appl. Phys. Lett. **69**, 3146 (1996).

[7]N. Bloembergen, IEEE J. Quantum Electron. **QE–10**, 375 (1974).

[8]T. Schwarz-Selinger, D. G. Cahill, S. C. Chen, S. J. Moon, and C. P. Grigoropoulos, Phys. Rev. B **64**, 155323 (1999).

[9]A. K. Burnham, M. Runkel, S. G. Demos, M. R. Kozlowski, and P. J. Wegner, Proc. SPIE **4134**, 243 (2000).

[10]T. M. Stephan, B. Van Zyl, and R. C. Amme, Proc. SPIE **1848**, 106 (1993).

[11]A. E. Siegman, in *DPSS Lasers: Applications and Issues*, OSA TOPS Vol. 17, edited by M. W. Dowley (Optical Society of America, Washington D.C., 1998), pp. 184–199.

[12]M. V. Klein, *Optics*, 2nd ed. (Wiley, New York, 1986).

[13]A. Ben-Yakar, A. Harkin, J. Ashmore, M. Shen, E. Mazur, R. L. Byer, and H. A. Stone, Proc. SPIE **4977**, 335 (2003).

[14]J. M. Liu, Opt. Lett. **7**, 196 (1982).

[15]J. Bonse, J. M. Wrobel, J. Kruger, and W. Kautek, Appl. Phys. A: Mater. Sci. Process. **72**, 89 (2001).

[16]P. Rudolph, J. Bonse, J. Krüger, and W. Kautek, Appl. Phys. A: Mater. Sci. Process. **69**, S753 (1999).

[17]M. Lenzner, J. Krüger, W. Kautek, and F. Krausz, Appl. Phys. A: Mater. Sci. Process. **68**, 369 (1999).

[18]S. Preuss, A. Demchuk, and M. Stuke, Appl. Phys. A: Mater. Sci. Process. **61**, 33 (1995).

[19]S. Nolte, C. Momma, H. Jacobs, A. Tünnermann, B. N. Chichkov, B. Wellegehausen, and H. Welling, J. Opt. Soc. Am. B **14**, 2716 (1997).

[20]T. Q. Jia, Z. Z. Xu, X. X. Li, R. X. Li, B. Shuai, and F. L. Zhao, Appl. Phys. Lett. **82**, 4382 (2003).

[21]P. R. Herman, R. S. Marjoribanks, A. Oettl, K. Chen, I. Konovalov, and S. Ness, Appl. Surf. Sci. **154**, 577 (2000).

[22]B. A. Nechay, U. Siegner, M. Achermann, H. Bielefeldt, and U. Keller, Rev. Sci. Instrum. **70**, 2758 (1999).

[23]P. Audebert, S. Guizard, K. Krastev, P. Martin, G. Petite, A. D. Santos, and A. Antonetti, Phys. Rev. Lett. **73**, 1990 (1994).

[24]R. H. Doremus, *Glass Science*, 2nd ed. (Wiley, New York, 1994).

[25]G. W. McLellan and E. B. Shand, *Glass Engineering Handbook*, 3rd ed. (McGraw-Hill, New York, 1984).

[26]F. Vidal, S. Laville, B. Le Drogoff, T. W. Johnston, M. Chaker, O. Bar-thélemy, J. Margot, and M. Sabsabi (Annual meeting of OSA - Optical Society of America, 2001).

[27]A. Salleo, T. Sands, and F. Y. Génin, Appl. Phys. A: Mater. Sci. Process. **71**, 601 (2000).

[28]A. M. Komashko, M. D. Feit, A. M. Rubenchik, M. D. Perry, and P. S. Banks, Appl. Phys. A: Mater. Sci. Process. **A69**, S95 (1999).

[29]T. Plettner, Ph.D. thesis, Stanford University, 2002.

[30]L. Shah, J. Tawney, M. Richardson, and K. Richardson, IEEE J. Quantum Electron. **40**, 57 (2004).

[31]A. E. Wynne and B. C. Stuart, Appl. Phys. A: Mater. Sci. Process. **76**, 373 (2003).